Review

Microfluidic DNA amplification—A review

Yonghao Zhang*, Pinar Ozdemir

Department of Mechanical Engineering, University of Strathclyde, Glasgow, G1 1XJ, UK

ARTICLE INFO

ABSTRACT

The application of microfluidic devices for DNA amplification has recently been extensively studied. Here, we review the important development of microfluidic polymerase chain reaction (PCR) devices and discuss the underlying physical principles for the optimal design and operation of the device. In particular, we focus on continuous-flow microfluidic PCR on-chip, which can be readily implemented as an integrated function of a micro-total-analysis system. To overcome sample carryover contamination and surface adsorption associated with microfluidic PCR, microdroplet technology has recently been utilized to perform PCR in droplets, which can eliminate the synthesis of short chimeric products, shorten thermal-cycling time, and offers great potential for single DNA molecule and single-cell amplification. The work on chip-based PCR in droplets is highlighted.

© 2009 Elsevier B.V. All rights reserved.

Contents

1. Introduction

The microfluidic technology associated with micro-total-analysis systems (μTAS), or lab-on-a-chip, has been developing rapidly and is set to revolutionize the chemical, pharmaceutical, healthcare and food industries. The global market for microfluidic technology is growing at a great pace and is estimated to be worth US$6.2 billion by 2011 [1]. Microfluidic devices can offer many advantages including quick analysis results, high-throughput and low consumption of reagents. In addition, the energy required for device fabrication and operation can be significantly reduced, which is particularly appealing when the world is experiencing an energy shortage. The microfluidic device appeared as early as 1975, when the first gas chromatograph was fabricated on a single silicon wafer [2]. The polymerase chain reaction (PCR) process is a technique first developed in 1984 by Kary Mullis for amplifying DNA [3]. It has since been widely used in biomedical research laboratories, and revolutionized many life science applications and related areas, including clinical diagnoses, and medical, biological and forensic analyses [4–7]. However, development of microfluidic PCR devices started much later in the early 1990s until the concepts of μTAS and lab-on-a-chip were proposed to take advantage of microfluidic devices for biological and chemical analyses [8].

* Corresponding author at: Department of Mechanical Engineering, University of Strathclyde, 75 Montrose Street, Glasgow, G1 1XJ, UK. Tel.: +44 141 5482854; fax: +44 141 5525105.
E-mail address: yonghao.zhang@strath.ac.uk (Y. Zhang).

Conventional PCR devices need to heat up and cool down, not only the PCR mixture but also the whole chambers, so the thermal mass is large, which leads to lengthy PCR reactions: typically 1–2 h. However, recent research showed that a very short time for both denaturation and annealing is required, to allow the sample to achieve equilibrium temperature [9]. Therefore, the time commonly used in conventional PCR (20–30 s for denaturation or annealing) can be significantly reduced. In addition, the conventional PCR will have a high consumption of expensive reagents, with a preference for amplifying short fragments and producing short chimeric molecules. Sample preparation and post-PCR analysis have to be done off-line, which makes it difficult to be integrated into a lab-on-a-chip system. These problems are amenable to recently developed microfluidic technologies. For example, microfluidic PCR can achieve rapid heat transfer, due to a large surface-to-volume ratio and fast mixing can be achieved by diffusion, due to its small dimension. At the same time, sample handling, detection, mixing, and separation can also be integrated into a single chip. Moreover, the thermal-cycling time will be significantly reduced, because of the swift thermal responsiveness of the sample to the surrounding environment and the PCR mixture will be exposed to more uniform temperatures during the PCR process, thereby enhancing the yield. A further attractive feature of miniaturized PCR is its portability, making it useful for in-the-field detection and analysis. However, interactions between the surface and the sample/reagent will lead to PCR inhibition and carryover contamination, which are two major problems associated with microfluidic PCR, due to its large surface/volume ratio. These problems can be prevented by introducing microdroplet technology, so that PCR occurs in droplets, which can eliminate sample/reagent surface adsorption and carryover contamination. With microdroplet technology, PCR in droplets can also prevent recombination between homologous gene fragments during PCR, so the synthesis of short chimeric products can be eliminated. PCR in droplets provides a convenient way for single-molecule and single-cell amplification.

Any review of this diverse multidisciplinary field needs to be selective, providing only a snapshot of the technologies being developed. In this short article, we cannot hope to cover all the available work related to microfluidic DNA amplification, but we will attempt to pick out some of the most important and exciting recent developments in continuous-flow microPCR and microfluidic PCR in droplets. Since the performance of continuous-flow microPCR strongly depends on optimization of the device design and operating flow rates, we will briefly discuss the essential flow physics for the proper use of many powerful commercial computational packages, aiming to help researchers who are not familiar with fluid dynamics and heat transfer. Device optimization and easy operation are particularly important in the future to enable users to adopt the microfluidic technology. Extensive coverage of this field, including materials, fabrication techniques, system integration and applications, can be found in many recent review articles, e.g., [5,7,10–14].

2. Continuous-flow microPCR chips

Currently, the chip-based microPCR devices can be classified into two distinct types: well-based PCR chips, e.g., [8,15–18] and continuous-flow PCR chips, e.g., [19–24]. In well-based PCR, the PCR mixture is injected into the well and then the whole chip, including the sample, is heated and cooled through specific thermal-cycling temperatures. Therefore, the well-based PCR devices have large total thermal mass, which creates unwanted thermal inertial effects, leading to a long thermal-cycling time. In contrast, continuous-flow microPCR moves the sample through fixed temperature zones to achieve the required thermal-cycling.

This approach has a smaller thermal inertia, because only the PCR mixture needs to be heated and cooled, rather than the entire chip. This allows rapid thermal-cycling and also consumes less energy, making the system more amenable to portable applications and integration into μTAS.

Continuous-flow microPCR chips have many different designs: e.g., oscillatory devices, e.g., [25–27], closed-loop devices, e.g., [28–30], and fixed-loop devices, e.g., [19,20,23,24,31,32]. In oscillatory PCR systems, the sample is shunted back and forth between the chambers that are held at different temperatures. In closed-loop PCR chips, a thermo-siphonic effect is utilized to move the sample around a fixed circuit. In both designs the number of thermal cycles can be flexible, whereas the number of cycles in a fixed-loop system must be determined at the fabrication stage.

Continuous-flow PCR was first performed in a capillary-based device. In 1994, Nakano et al. [19] developed the first capillary-based continuous-flow PCR device, which used a Teflon capillary with an internal diameter of 500 μm. In one thermal cycle, the PCR mixture went through a 20-mm-long denaturation zone with a temperature of 94 °C, a 30-mm-long annealing zone with a temperature of 50 °C and a 100-mm-long extension zone at 72 °C. In comparison with the commercial thermocycler, a 50% amplification yield was achieved with only 10% of the processing time, i.e. 12–18 min. Another novel capillary-based PCR device was reported by Friedman and Meldrum [33], which used a thin film of indium–tin oxide (ITO) covering the exterior of the capillary functioning as both heater and temperature sensor. Because the thin film is optically transparent for fluorescence monitoring, it has potential for real-time PCR. Chiou et al. [21] proposed a similar design, with a 1-mm-internal-diameter capillary filled with oil. The PCR mixture was injected as a 1 μL droplet, to cycle through three temperature zones for 30 times in 23 min, with 78% amplification efficiency for a 500-base pair product. With further optimization, this PCR device could complete 30 thermal cycles in 2.5 min. To eliminate carryover contamination between sequential runs, a washing step between sequential injection of samples was adopted in capillary-based reusable PCR devices [34,35]. Although these capillary-based PCR devices have demonstrated the potential of a continuous-flow device for a high-speed and high-yield PCR with a flexible cycling number, they are not chip-based, which makes them difficult to develop further into an integrated microfluidic system.

The first chip-based continuous-flow microPCR was developed in 1998 by Kopp et al. [20], where a 40-μm deep and 90-μm wide channel was etched in a Corning 0211 glass chip, with a total length of 2.2 m for 20 cycles (see Fig. 1). The device capability was demonstrated by amplifying a 176-base pair DNA fragment at the flow rates from 5.8 to 72.9 nL/s, corresponding to a PCR time of 18.7–1.5 min for 20 cycles. This pioneering work has since inspired the development of a broad range of chip-based microfluidic PCR devices, e.g., [25,32,36–42].

Schneegaß et al. [37] built a 25-cycle silicon-glass PCR chip, which had integrated heaters and temperature sensors, fabricated on-chip using integrated circuit manufacturing technology. West et al. [29] reported a rotationary PCR chip, so that the cycle number was flexible. The motion of the fluid sample in an annular microchannel was driven by an AC magnetic field, which exploited the conductive nature of the electrolyte. This magnetic-field pumping method has also been adopted by Sun et al. [44]. Another rotary PCR chip design with the integrated heaters, which can perform both spatial and temporal cycling, was developed by Liu [28]. Sun et al. [38] have developed a 30-cycle continuous-flow PCR device with the integrated ITO heaters, thus making the device optically transparent. Obeid and Christopoulos [42] combined a continuous-flow reverse transcription PCR (RT-PCR) with a laser-induced fluorescence (LIF) detection system. Obeid et al. [41] presented a device capable of the reverse transcription of RNA, prior to its amplification
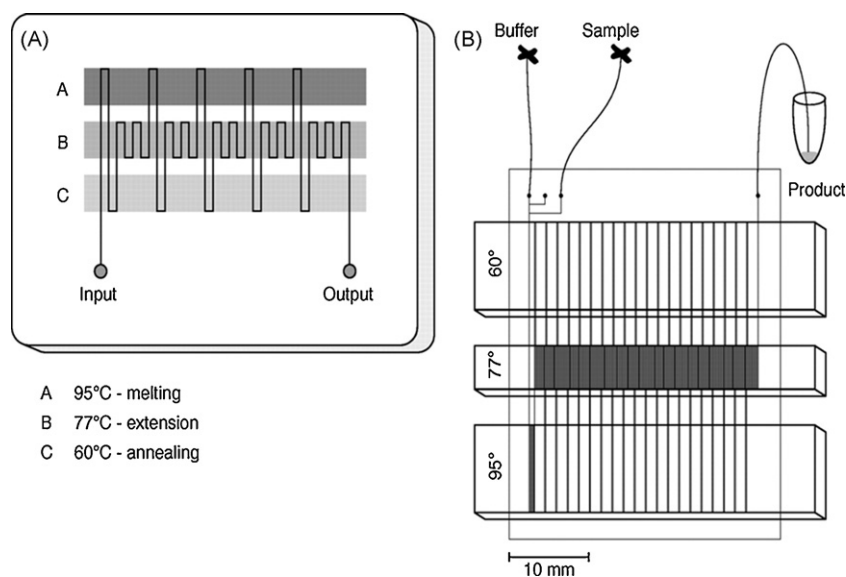
Fig. 1. Schematic diagram of continuous-flow PCR chip: (A) layout of three temperature zones for PCR thermal cycles which are maintained at 95, 77, and 60 °C. A pressure pumping method is used to inject the sample through a single channel etched into the glass chip. (B) Device layout: three inlets on the left side of the device and one outlet on the right: with only two inlets are used to inject both the sample and buffer. (From M.U. Kopp, A.J. deMello, A Manz, Science 280 (1998) 1046. Reprinted with permission from AAAS.).

in a 40-cycle serpentine channel. The device was fabricated with the outlets at the cycle numbers of 20, 25, 30, 35, and the full 40. In addition, the researchers were able to demonstrate amplification with plug flow, thus reducing the amplification volume to 2 μL per amplified sample. A 30-cycle continuous-flow microPCR device was reported [40], where the miniature pumps and valves were used, the heating was provided by the embedded ITO heaters, and the temperature was controlled via the integrated platinum sensor.

Similar to the Rayleigh–Benard cell for PCR [45], Braun et al. [46] used laser to generate a temperature gradient, in order to induce density variation to drive the sample through different temperature zones for PCR processing. An averaged velocity of 2.5 mm/s for a temperature gradient induced flow was achieved in a rotary PCR chip [22]. Crews et al. [32] proposed a continuous-flow thermal gradient PCR, with each cycle consisting of temperature spikes to denature and anneal by passing through the narrow channel, then a moderate thermal ramp through the extension temperature in the wide channel, where the authors achieved a high yield and specificity amplification for a 40-cycle PCR in less than 9 min (see Fig. 2).

Hashimoto et al. [47] developed a device in which the different temperature zones were separated into the four quadrants of a rectangular substrate. By fabricating a 20-loop spiral microchannel through each temperature zone repeatedly, the moving fluid was able to obtain the required temperatures and thermocycling times. Similarly, a quadrant heating/spiral channel continuous-flow microPCR device was developed by Wang et al. [23], to perform Sanger thermal cycle sequencing reactions.

The isothermal regions are significantly affected by thermal "cross-talk" [48], and the multiple isolated temperature zones greatly complicate the design of the continuous-flow PCR [32]. However, with improved insulating methods in the fabricated devices, better thermal separation between the several temperature zones is possible [37,47,49]. There are other approaches to reducing time for heating up and cooling down the sample. For example, Li et al. [48] built a device, whose 20-cycle serpentine microchannel was narrower in the regions between the three temperature zones, thus reducing the inter-temperature transition time [48].
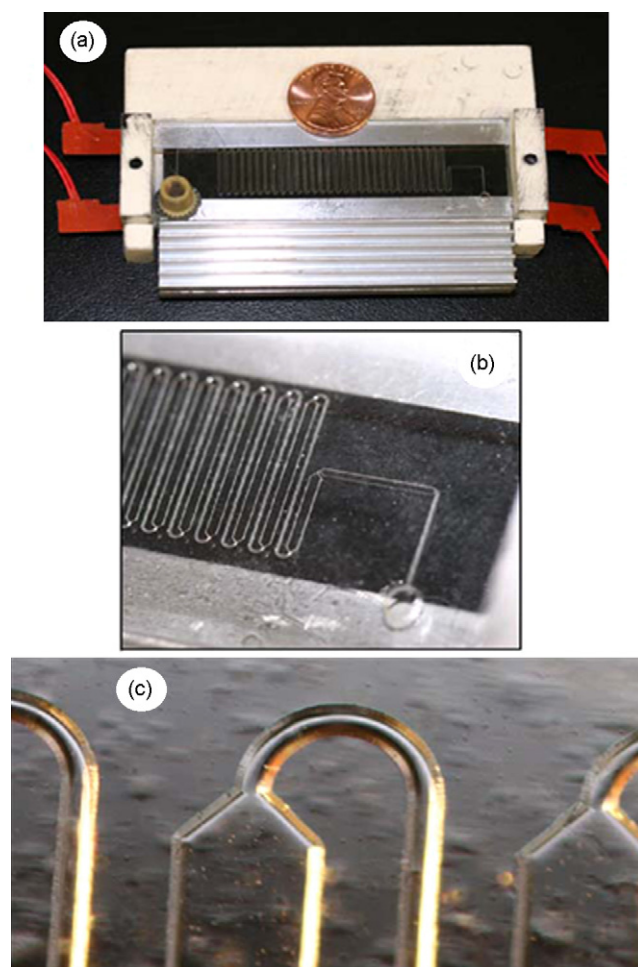

Fig. 2. (a) The continuous-flow thermal gradient PCR chip. (b) The serpentine channel has a linear temperature gradient, where rapid temperature change is achieved in a narrow channel, while slow ramp rates are obtained in a wide channel. (c) The smooth and curved glass channel surface. (With kind permission from Springer Science: Biomedical Microdevices, Continuous-flow thermal gradient PCR, 10 (2008) 187, N. Crews, C. Wittwer, B. Gale, Fig. 3.).

Table 1
Summary of the continuous-flow PCR chips.

Device	Layout	Heaters	Demonstration	Other features
[20]	Fixed-loop with 20 cycles		Amplification of 176-base pair DNA fragment as low as 90 s for 20 cycles	First on-chip continuous-flow PCR
[37]	Fixed-loop with 25 cycles	Integrated heaters	Amplification of 700-base pair fragment in less than 30 min for 25 cycles	Proposed a liquid/liquid two phase PCR
[29]	Closed-loop design			Magnetohydrodynamic force used to pump fluid
[29]	Closed-loop design	Integrated heaters	Amplification of 199-base pair DNA fragment in 40 min	On-line detection of fluorescence level
[38]	Fixed-loop with 30 cycles	Integrated ITO heaters	450-Base pair fragment amplified in 19 min for 30 cycles	On-line fluorescence monitoring system
[25]	Oscillatory chip	Integrated heaters		Numerical simulation for device optimal design and operation
[41,42]	Fixed-loop with multiple cycles 20, 25, 30, 35, and 40		Amplification of 230-base pair fragments for 30 cycles in only 6 min	DNA and RNA application; laser-induced fluorescence detection system
[40]	Fixed-loop with 30 cycles	Integrated ITO heaters	1460-Base pair fragments successfully amplified in 60 min for 30 cycles	
[47]	Fixed-loop with 20 cycles		500- and 997-base pair fragments amplified in 1.7 and 3.2 min for 20 cycles, respectively.	Numerical simulation for determining device optimal flow rates
[51]	Fixed-loop with 50 cycles		113-Base pair fragment amplified in 40 min for 50 cycles	A method proposed to prevent bubble generation; laser-induced fluorescence detection system
[23]	Fixed-loop with 20 cycles		Able to amplify up to 632-base pair fragments in 14.6 min for 20 cycles.	Coupled with a solid-phase reversible immobilization chip
[48]	Fixed-loop with 20 cycles		Successful amplification of 90-base pair fragment	Numerical simulation for device optimal design
[44]	Closed-loop design		Amplification of 500-base pair fragment in 13.5 min for 30 cycles.	Magnetohydrodynamic force used to pump fluid
[50]	Fixed-loop with 30 cycles		290-base pair fragment amplified in 18.7 min for 30 cycles.	Coupled with 13 cycles for an allele-specific ligation detection reaction
[52]	Oscillatory PCR chip		Demonstrated to determine the threshold cycle number for their device	Proposed a parallel design to increase throughput; on-line optical detection system to monitor fluorescence level
[32]	Fixed-loop with 30 cycles	Integrated heating/cooling elements	For 40 cycles, less than 9 min required to amplify 108/181-base pair fragments with high yield and specificity	Narrowing/widening channels to manipulate temperature gradient

A broad range of applications of microfluidic PCR have been reported. For example, Hashimoto et al. [50] coupled an allele-specific ligation detection reaction to continuous-flow PCR in a polycarbonate chip and successfully detected low-abundant DNA point mutations. Nakayama et al. [51] demonstrated real-time amplification detection using TaqMan technology. A micro oscillating-flow PCR chip was developed by Wang et al. [23], where the PCR mixture was injected into the channel and flowed through the three temperature zones in the main microchannel in an oscillating manner. A 1 μL PCR mixture with a standard Human Papilloma Virus-DNA (HPV-DNA) sample inside was successfully amplified, with a processing time of about 15 min.

Increasing throughput has attracted strong research interest, e.g., Frey et al. [52] invented a single actuator to deflect all pumping membranes, so the sample can be driven to move through three temperature zones, thus parallel multiple channels, which simultaneously perform PCR reactions, can greatly increase throughput. Moreover, 72 parallel 450-pL RT-PCRs have also been performed in a microfluidic chip [53]. The features of the above continuous-flow PCR chips are summarised in Table 1.

3. PCR inhibition and carryover contamination

For continuous-flow microPCR, PCR inhibition becomes a major challenge, because PCR components are more likely to be adsorbed to the surface due to large surface/volume ratio. The adsorption of sample and reagents will also cause carryover contamination. Gonzalez et al. [54] investigated the adsorption of PCR components in the capillary tubes with different polymeric surfaces. The authors found that increasing the tube length or reducing the sample vol-

ume had the most significant effect on PCR inhibition. The reason is that the surface area is sufficiently large to adsorb all the PCR components, which is often true for continuous-flow microPCR, due to the large surface/volume ratio and small amount of sample and reagents. Kolari et al. [55] studied PCR inhibition on commonly used microfluidic materials, where the effects of a minor inhibition were observed for native silicon and an SF6 etched surface without oxidation, while strong inhibition for fluorocarbon-coated silicon was found. However, Wang et al. [56] found that the native silicon surface could adsorb the TaqMan real-time PCR label. PCR inhibition on many different materials has also been reported, e.g., strong PCR inhibition was observed on silicon and silicon nitride (SiN) surfaces [15,57–64]. More work is required to systematically classify the biocompatibility of microfluidic materials.

To prevent PCR inhibition and carryover contamination, various measures have been taken to minimise surface adsorption of DNA and PCR reagents. Schneegaß et al. [37] proposed a material treatment of the channel surface with a silanizing agent, such as hexamethyldisilazane (HMDS), before the injection of the PCR mixture, so the hydrophobic material surface of the silicon/glass was modified to enhance surface biocompatibility. Similarly, Kim et al. [65] reported a surface modification method that prevented the hydrophobic PDMS surface from adsorbing enzymes by adding polyvinylpyrrolidone (PVP) to the PCR mixture. Polymer coating was proposed using 2-methacryloyloxyethyl phosphorylcholine (MPC) with a silane coupler, to prevent the adsorption of DNA on the intact surface of the PDMS microchannels [40]. Prakash et al. [66] applied an SU8-Teflon coating to modify the contact angle of a sessile Taq droplet to reduce adsorption. Passivation strategies were developed by Schneegaß and Kohler [36] to partially eliminate

sample DNA and reagent surface adsorption and carryover. However, a washing step between samples was needed. A dynamic passivation method was investigated by Xia et al. [67], using polyethylene glycol (PEG) or PVP, to enhance PCR yields. Moreover, Chen et al. [68] reported a bidirectional flow thermocycling system which took advantage of the low surface area/volume ratio of a stationary reactor to minimise surface adsorption of DNA and reagents. One of the most effective means of eliminating surface adsorption and carryover contamination has to be performing PCR in droplets.

4. PCR in droplets

A lengthy PCR process caused by high thermal inertia has been dramatically shortened by continuous-flow microPCR devices. However, in addition to sample/reagents surface adsorption due to a large surface/volume ratio, a new problem occurs, which is caused by the parabolic velocity profile of the channel flowfield. Because the velocity profile is parabolic for a pressure pumping method, the PCR sample will experience significantly different times for PCR processing, depending on the sample's cross-sectional location in the channel. Close to the surface, the PCR components can spend significantly more time being processed than those located in the centre of the stream, which causes problem for flow rate optimization. Moreover, single-phase microPCR will also have the two problems suffered by conventional PCR: the preference for amplifying short fragments and the production of short chimeric molecules [69]. These problems are amenable to microdroplet technology.

Recently, the microdroplet technology has been applied in continuous-flow microPCR, where the PCR effectively occurs within droplets, so that not only PCR inhibition but also carryover sample contamination will be eliminated. In comparison with conventional continuous-flow microPCR devices, which use a single aqueous phase, the droplet technology can further reduce thermal mass and thus shorten the thermal-cycling process. As each sample and reagents are confined in a microdroplet, any local temperature variations will be small and each droplet can achieve a more uniform temperature. In addition, the PCR mixture confined in a droplet will have the same residence time. The device can be used with predetermined amounts of target nucleic acids, with potential applications to amplify a single DNA molecule or single cells, with the nucleic acids from one cell being amplified inside one droplet. Such an approach could greatly assist in transforming our understanding of how disease-associated transcripts relate to disease progression. As the samples are contained in droplets, they could be detected and subsequently sorted on the chip itself, which is particularly important for an integrated lab-on-a-chip system. For a conventional PCR chip, amplification of each DNA template would require a separate run, while the droplets can act as individual reactors containing many DNA templates and being amplified individually within the droplets, moving through the same PCR cycles. Microdroplet technology is currently under rapid development: research progress and application of this technology can be found in the recent review articles [70–73]. A schematic diagram of microfluidic PCR in droplets can be seen in Fig. 3, with a summary of the associated advantages.

With conventional PCR devices, droplets have been used to generate DNA libraries, including genomic libraries and cDNA libraries. Droplet-based PCR has recently been applied to sequencing, assessing genetic variations and high-throughput screening of transcription factor targets [74–80]. Conventional PCR tends to amplify short fragments in preference to larger ones. In addition, the recombination between homologous regions of DNA leads to artifactual fragments. With encapsulation of genes in a water droplet immersed in an immiscible oil carrier phase, template fragments are confined in the small aqueous droplets and amplified by PCR in isolation, which alleviates the above problems and enables the
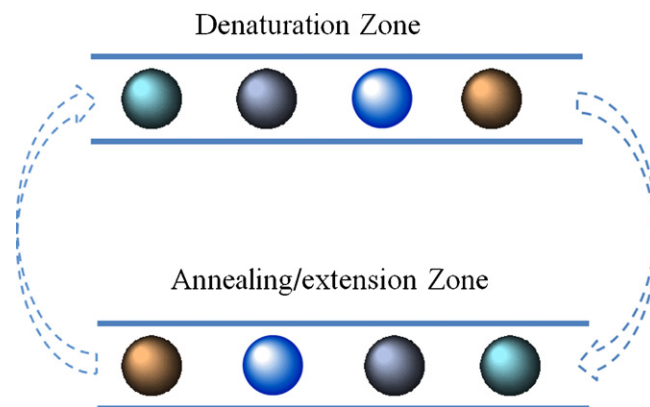

Fig. 3. An illustration of microfluidic PCR in droplets: the PCR mixture is contained in discrete droplets, moving through different temperature zones in the microchannels for DNA denaturation, annealing/extension. The microfluidic PCR in droplets has many advantages compared with conventional PCR and single-phase microfluidic PCR, e.g., elimination of carryover contamination between successive samples, adsorption at the surface, and diffusional dilution of samples; prevention of the synthesis of short, chimeric products and other artifacts; rapid thermal response for fast PCR process; low consumption of reagents; easy integration as a function of a µTAS. In addition, individual droplets can contain different PCR samples, so that it is particularly suitable for single-cell and single-molecule amplification.

use of small amounts of template DNA and high numbers of PCR cycles [69,81]. Because each droplet only contains a single, or at most a few, template DNA molecules, this prevents recombination between homologous or partially homologous gene fragments during PCR, thus eliminating the synthesis of short, chimeric products and other artifacts. In addition, the competition between fragments of different lengths is also reduced, thus diminishing the bias for amplifying smaller fragments [69]. Since water-in-oil droplets are stable at temperatures higher than 90 °C, it is a very efficient and simple way to perform parallel amplification of single DNA or RNA molecules. These features of PCR in droplets will be a great stimulus to develop droplet-based continuous-flow microPCR devices. Conventional PCR devices using droplets provides a high-throughput method for DNA sequencing, interested readers can refer to the recent review papers [69,71] for more information.

To date, a single-phase containing PCR components is used to fill the channel in most continuous-flow microPCR devices, which can lead to carryover contamination between successive samples, adsorption at the surface, and diffusional dilution of samples, e.g., [20]. These problems can partially be overcome by making use of immiscible liquids to isolate the sample slugs from each other [82]. For example, Curcio and Roeraade [83] developed a high-throughput microfluidic PCR device, using a 15-m-long Teflon tube coiled to cycle through three temperature zones, where samples/reagents were introduced as separate aqueous segments in a continuous-flow of an immiscible organic liquid. An intermediate water plug was injected between two consecutive samples to reduce carryover between samples.

Another interesting approach to preventing sample contamination is to use plugs of air to separate aqueous sample plugs [31,41,42]. However, the surface still has contact with samples and reagents, so needs to be treated to eliminate adsorption of sample/reagents and subsequent transfer between samples. However, it is difficult to totally eliminate carryover contamination with surface treatment [31]. As interaction between the PCR mixture and the surface is a key factor that inhibits the PCR process, microdroplet technology can help to eliminate this undesired contact between sample and surface.

Nisisako et al. [84] have demonstrated that droplets of an aqueous phase can be dispersed into an immiscible oil phase. Each

droplet potentially represents a transportable individual reaction volume that does not exchange material with its surroundings. The droplets will only be in contact with the surface when required, and then only at specific locations. Droplet-based systems can therefore avoid the problems of adsorption, cross-contamination, and diffusional dilution associated with single-phase microfluidic systems. Musyanovych et al. [85] reported the generation of water-in-oil nanodroplets with a diameter of 100–300 nm for performing single DNA molecule PCR. A single RNA molecule was also successfully detected by Nakano et al. [86], using continuous-flow PCR in droplets for single-molecular amplification, which demonstrates the great potential of droplet technology in amplifying a single-molecule template.

Dorfman et al. [87] developed a continuous-flow PCR device using droplets to encapsulate the PCR components. The droplets were at the order of 1 μL, and a 4.5-m-long PEA capillary (i.d. 800 μm) was coiled around a cylinder, to achieve 35 thermal cycles. The authors successfully amplified a 572-base pair DNA fragment of Litmus 28i. The system was further improved to integrate sample preparation and optical detection [88]. A simple droplet-based PCR device using magnetic transportation was reported by Ohashi et al. [18], where aqueous droplets containing hydrophilic magnetic beads and the applied magnetic field was used to manipulate the transportation of droplets through different temperature zones in a flat-bottomed tray-type reaction chamber. Gonzalez et al. [54] introduced droplets in their rotary PCR devices, using a Teflon capillary tube, and demonstrated robust detection of the low-copy transcript CLIC5 from 18 cells per microliter in cultured lymphoblasts, which indicates the potential for development of an integrated system for continuous gene expression directly from cell suspensions.

However, these droplet-based PCR were not performed on-chip, so it is difficult for system integration. Mohr et al. [24,43] successfully coupled microdroplet technology with a continuous-flow microPCR chip (see Fig. 4a). Their schematic diagram of PCR chip design can be seen in Fig. 4b. The chip was fabricated from a polycarbonate sheet, using a precision milling machine and the channels were sealed with a 100 μm thick acetate foil. The total thermocycles were 32 and the length of one complete thermal cycle was 63 mm. The channels were 500 μm wide and 400 μm deep. The aqueous droplets were generated at the channel entrance with the dimensions of 200 μm wide and 200 μm deep, filled with an oil phase (see Fig. 4c). The reported droplet size was between 100 and 155 μm in diameter, so that the volume of a droplet was at the order of 5 nL. An optical system was established to monitor the fluorescence level after each thermal cycle, which enables quantitative real-time PCR measurements. The successful amplification of a 60-base pair fragment from the RNase P gene was achieved.

Beer et al. [89,90] have developed picoliter droplets for PCR amplification, with real-time measurement of fluorescence detection (see Fig. 5). The monodisperse picoliter aqueous droplets were generated at a T-junction and isolated from the surface and each other by an immiscible oil-phase carrier fluid. The droplets were stopped on-chip by an off-chip valving system, to perform thermal cycles. With their system, only 18 cycles were required for single-copy real-time detection, using Taqman-based FRET probes. The system was used for reverse transcription PCR (RT-PCR), to amplify cDNA from a complimentary RNA template. It showed the great potential of droplet technology for the detection of single-copy target nucleic acids from a complex environment. However, this is a well-based continuous-flow PCR chip so that the whole chip, including fluids, needs to be heated up and cooled down for each thermal cycle, which leads to lengthy PCR process. Another well-based PCR chip, using a magnet to manipulate droplets containing magnetic beads, was recently reported [91], which was convenient for separation and fusion of droplets.
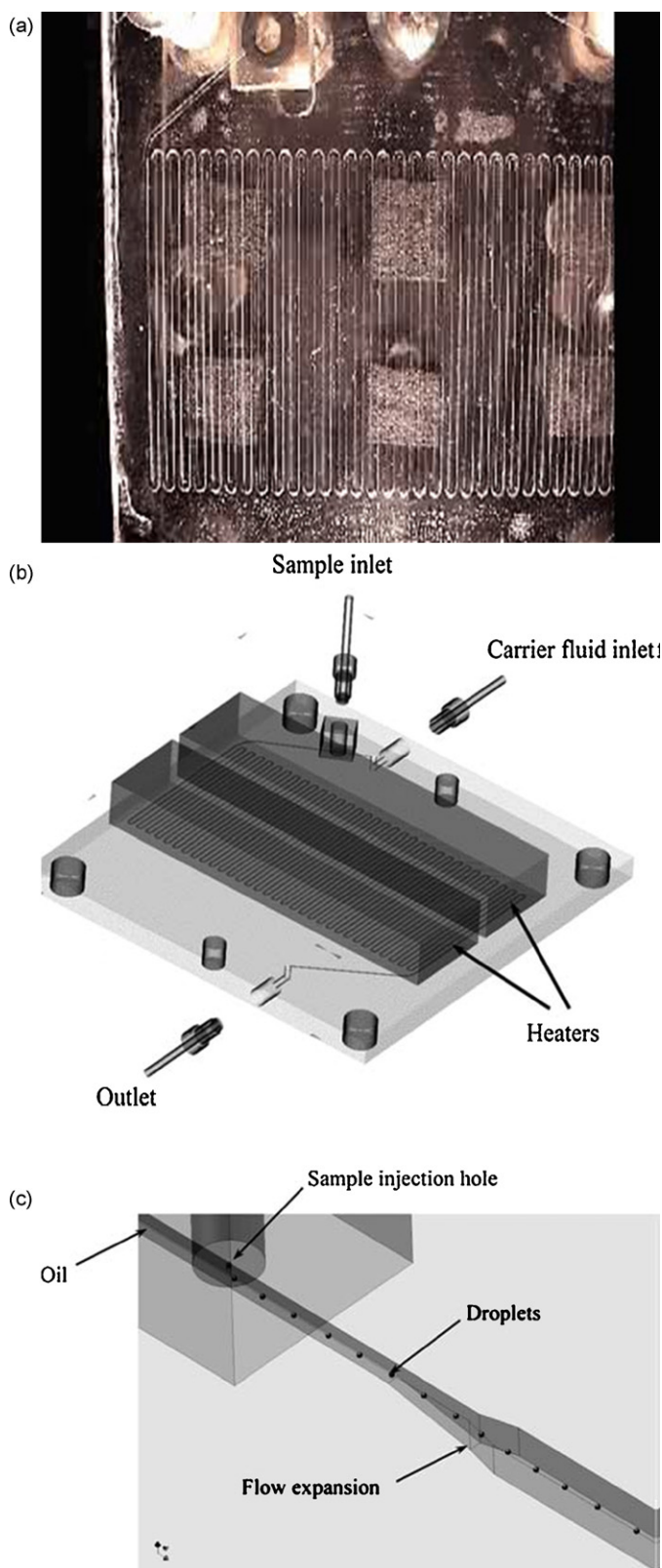

Fig. 4. (a) The continuous-flow microPCR chip with PCR sample and reagents contained in droplets. (b) Layout of the PCR chip. (c) The aqueous droplets are generated by the imposed shear force from the carrier oil phase. (With kind permission from Springer Science: Microfluidics and Nanofluidics, Numerical and experimental study of a droplet-based PCR chip, 3 (2007) 611, S. Mohr et al., Figs. 1, 2 and 4.).
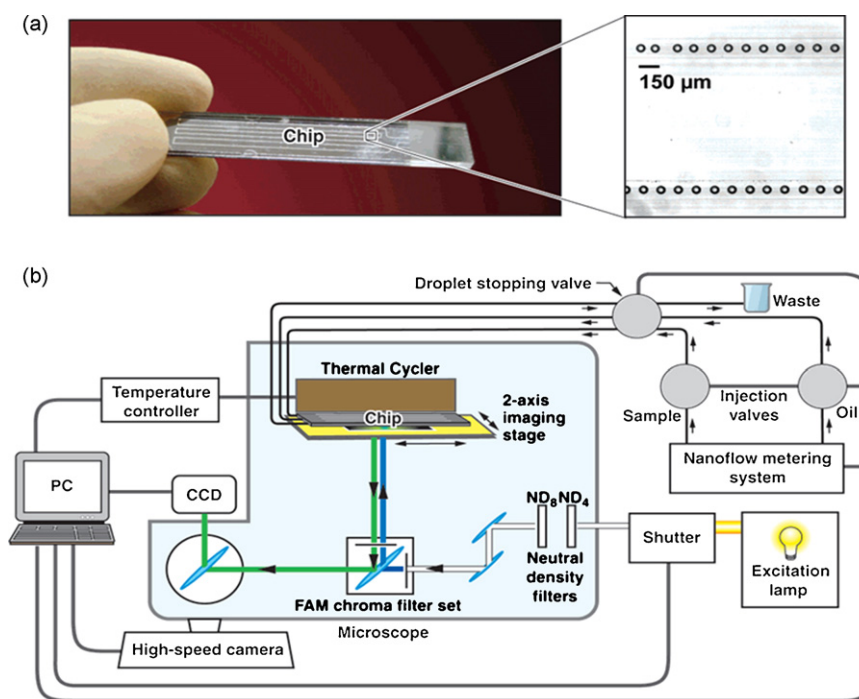
Fig. 5. Schematic diagram of the on-chip RT-PCR device: (a) the fused-silica device with an inset of monodisperse ~70-pL droplets trapped and ready for subsequent PCR. (b) A schematic of the instrument. (Reprinted with permission from Beer et al. On chip single-copy real-time reverse-transcription PCR in isolated picoliter droplets, 80 (2008) 1854. Copyright 2009 American Chemical Society.).

A high-throughput chip-based continuous-flow PCR was reported by Kiss et al. [92] where millions of uniform picoliter droplets were generated on-chip in order to detect single-copy target nucleic acids from a complex environment. In addition, on-chip detection function to monitor fluorescence level within each droplet was integrated to provide real-time measurement. A 245-base pair adenovirus product was successfully amplified and quantified in 35 min at initial template concentrations as low as 1 template molecule/167 droplets. The chip layout and the droplet generation can be seen in Fig. 6.

Recently, Schaerli et al. [93] developed a novel radial design of continuous-flow PCR chip (see Fig. 7). The droplets were generated on chip and 34 thermal cycles were performed in only 17 min to amplify a DNA fragment with 85-base pairs. In addition, the temperatures of droplets were measured via fluorescence (rhodamine B) lifetime imaging inside the droplets, which utilized the known relation between the temperature and fluorescence lifetime. The high amplification efficiency indicates its potential for single-DNA molecule amplification in each droplet.

Although droplet-based continuous-flow microPCR chips are still at an early stage of their development, the recent work [24,43,89–93] have demonstrated the feasibility and great potential, particularly for high-throughput single-molecule and single-cell PCR. The current challenges are how to produce reliable monodispersed droplets and how to control droplet trajectories, and their interactions with the surface and each other. Considerable work on the novel design of droplet-based continuous-flow microPCR devices is required before their full potential can be realised. A summary of the current work on chip-based PCR in droplets is shown in Table 2.

5. Optimal design and operation

Research on the reaction kinetics of PCR has shown that the sample only needs to achieve equilibrium temperature for denaturation or annealing, which indicates that the PCR process can be significantly reduced and the time needed for extension will dominate each thermal cycle [9]. Therefore, continuous-flow PCR devices generally require considerable optimization for the device design and operation, in order to ensure the sample/reagents attain the appropriate temperatures with minimum residence times for denaturation, annealing, and extension. At the moment, the microfluidic PCR optimal design and operation still largely rely on the trial-and-error approach, which can be replaced by computer-aided design, exploiting powerful commercially available software such as FLUENT, ANSYS, CFD-ACE+. There are many advantages that numerical experiments can offer, e.g., three-dimensional temperature distribution, which is usually difficult to obtain by experimental measurement. In addition, the effects of different chip materials and layout, heating/cooling arrangements, fluid properties and flow rates can be easily examined.

Zhang et al. [94] used ANSYS, a finite element package, to optimize their continuous-flow PCR chip design. Their focus was on the effect of different materials on the heat transfer and temperature distribution, which is essential for PCR performance. Since glass and silicon have very different thermal conductivities (the thermal conductivity coefficient for silicon is $130 W/(m K)$, while it is $0.65 W/(m K)$ for glass), the temperature distribution in the flow channel is significantly affected by the chosen materials. However, the authors neglected the effect of moving fluid in the channel due to its small dimension. For a PCR thermal cycle, it is most important for the PCR sample to achieve optimal temperatures for denaturisation, annealing and extension. The temperature distribution in the flow channel, which depends on flow rates and fluid properties, should be examined in details.

Using ANSYS, Hashimoto et al. [47] also studied the effect of flow rate on the temperature distribution in the microchannel and found that the denaturation temperature could not be achieved at large flow rates. In their work, temperature distribution in every thermal cycle was assumed the same, so that only one thermal cycle was simulated. In addition, the temperature gradients were taken to be zero at the inlet and outlet of the chosen representative thermal cycle. These assumptions may be appropriate when the flow rate is sufficiently small, so that thermal development length
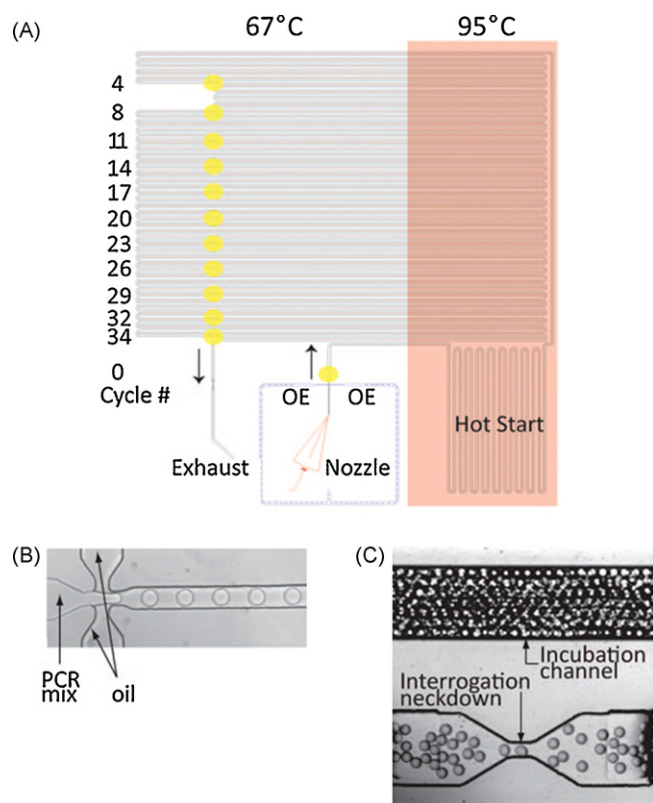
Fig. 6. The layout of PCR chip. (A) The temperature is set at 95 °C in the pink-shaded regions, and 67 °C in the other nonshaded regions. The regions highlighted in yellow is the detection zones with channel neckdowns, and the corresponding cycle numbers are noted on the left. The PCR mixture is injected in the nozzle which is highlighted in red, and the carry fluid oil is injected through the side nozzles acting as oil extractor (OE) which is in blue. (B) Droplet generation at the nozzle. (C) Uniform picoliter droplets in the downstream channel and flowing through one of the neckdowns. (Reprinted with permission from Kiss et al. High-throughput quantitative polymerase chain reaction in picoliter droplets, 80 (2008) 8975. Copyright 2009 American Chemical Society.). (For interpretation of the references to color in this figure legend, the reader is referred to the web version of the article.)
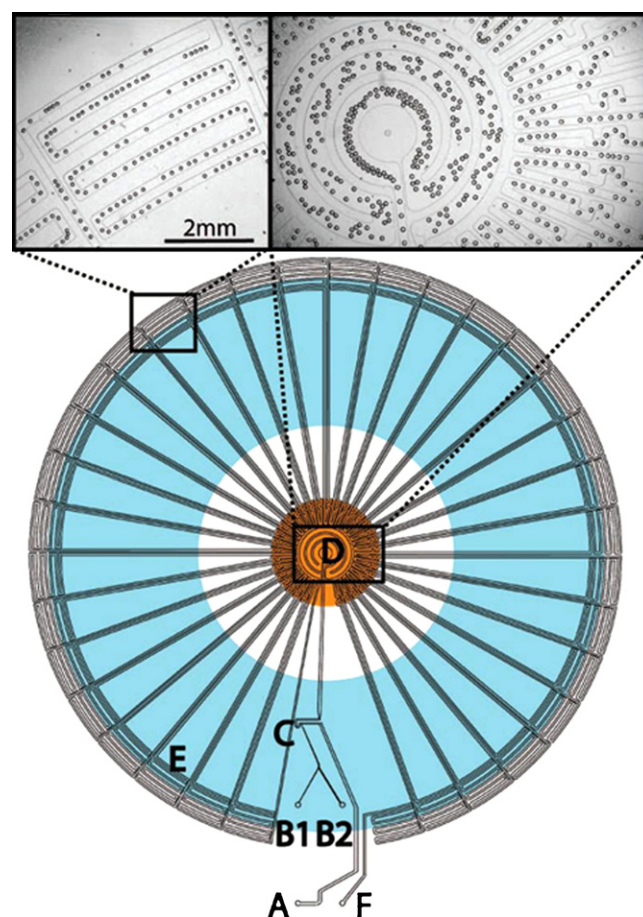

Fig. 7. The schematic diagram of the radial PCR device. The carrier fluid oil is injected at the inlet A and aqueous phase is injected at two inlet channels (B1 and B2), so that droplets are generated at a T-junction (C). The channels are 75 μm deep, and 500 μm wide in the hot zone (D) to ensure initial denaturation of the template. The channels are 200 μm wide in the periphery (E) where primer annealing and template extension occur. After 34 thermal cycles, the droplets are collected at the exit F. The heat is provided via the underlying copper rod (Ø: 1.2 cm) highlighted in orange, and the Peltier module (inner Ø: 2.7 cm, outer Ø: 5.5 cm) are used to adjust thermal gradient (blue area). (Reprinted with permission from Schaerli et al. Continuous-flow polymerase chain reaction of single-copy DNA in microfluidic microdroplets, 81 (2009) 302. Copyright 2009 American Chemical Society.). (For interpretation of the references to color in this figure legend, the reader is referred to the web version of the article.)

is considerably shorter than the length of the extension zone. Wang et al. [27] theoretically analyzed and numerically simulated the performance of a micro oscillating-flow PCR chip. In computational simulations, precautions are required to appropriately set up physical properties. For example, the viscosity and thermal conductivity depend strongly on temperature (e.g., the viscosity of pure water is 4.34×10^{-4} and 2.97×10^{-4} kg/ms at 65 and 95 °C, respectively, which is a significant variation). Therefore, in the

Table 2
On-chip PCR in droplets.

Device	Droplet generation	Detection	Efficiency/achievements	Other features
Mohr et al. [24,43]	Droplets (100–155 μm in diameter) generated at an integrated T-junction	On-line monitoring fluorescence level within each droplet	60-Base pair fragment from the RNase P gene amplified in about 8 min for 32 cycles	Numerical simulations carried out to optimize flow rates; Continuous-flow PCR chip
Beer et al. [89,90]	Droplets (averaged diameter of 51, 29, 31, 27 and 24 μm) generated at an integrated T-junction	On-line fluorescence detection within each droplet	The device used for RT-PCR	Well-based PCR chip
Kiss et al. [92]	Monodisperse droplets with 50-μm diameter generated by a focused flow at a cross-junction	On-line fluorescence detection within each droplet	A 245-base pair adenovirus product amplified and quantified in 35 min at initial template concentrations as low as 1 template molecule/167 droplets.	The device can produce millions droplets per hour and is able to perform single-molecule PCR; Continuous-flow PCR chip
Schaerli et al. [93]	Droplets generated on-chip at a T-junction		34 thermal cycles for only 17 min to amplify a DNA fragment with 85-base pairs	The temperatures of droplets were measured by fluorescence lifetime imaging inside the droplets; continuous-flow PCR chip with radial layout

simulation, we need to ensure that material properties are chosen to reflect the underlying physics.

Aided by a computational fluid dynamics (CFD) package (CFD-ACE+), Mohr et al. [24,43] assessed the effects of the flow rates and thermal resistances of different materials on the temperature distribution in the flow channel and the corresponding times for denaturation, annealing/extension. They found that temperature distribution in the moving fluid was greatly affected by both flow rates and material thermal properties. For a large flow rate, the temperature distribution pattern in each cycle can be different, which indicates that it is not appropriate to run a simulation on one single representative thermal cycle. To minimise the heating and cooling times, the carrier fluids with a low thermal mass are preferred.

Chen et al. [95] again used ANSYS to evaluate the temperature distribution in the chip including the moving fluid in the microchannel at a steady state, and investigated the effect of the flow rate on the amplification performance. Several steps were suggested to ensure three discrete uniform temperature zones, i.e. reducing the thickness of the chip substrate to decrease thermal capacity; using copper plates as heating elements to increase heat conductivity; making grooves between temperature zones to increase the resistance to lateral heat conduction between temperature zones. The simulation setup is similar to the work of Hashimoto et al. [47], but the authors have considered the material properties to be temperature-dependent.

Because flow behaviour at a small scale may not be the same as the conventional scale and may be different from intuitive expectation, understanding flow physics at a small scale becomes essential, which is also critical for the optimization of a microfluidic device design and operation. In the following section, we briefly cover basic flow physics for the microfluidic researchers, who are not familiar with fluid dynamics and heat transfer, to perform numerical experiments using commercially available computational packages.

6. Flow physics

6.1. Transport properties

Fluid is a matter that cannot remain at rest when it is subject to a shear force. The transport properties of fluid, such as viscosity, thermal conductivity and mass diffusivity, are most important to understand momentum, heat and mass transport. For the common fluids used in microfluidic PCR, including water, oil, and gas, the shear stress is linearly dependent on the strain rate, i.e.

$$\tau = \mu \nabla \boldsymbol{u}, \tag{1}$$

where τ is the shear stress, μ is the coefficient of viscosity and $\boldsymbol{u}$ is the velocity. These fluids are called Newtonian fluid. The coefficient of viscosity of a Newtonian fluid is a function of temperature and pressure. The viscosity of liquids decreases rapidly with temperature, while it increases insignificantly with pressure. Therefore, in the simulation, we need to make sure the viscosity is temperature-dependent. In the literature, a constant value of viscosity coefficient is commonly used in the simulation of continuous-flow PCR.

The heat flux is usually caused by a temperature gradient, which can be described by the Fourier's law:

$$\mathbf{q} = \kappa \nabla T \tag{2}$$

where $\mathbf{q}$ is the heat flux, T is temperature and κ is the coefficient of thermal conductivity. The thermal conductivity for both solid and fluid varies widely with temperature. Therefore, again, in setting up computational simulations, the temperature effect on this coefficient may be essential for accurate results. Silicon can have a thermal conductivity coefficient of two-order in magnitude as large as polymers and glass. It is preferable to use silicon near the heating sources to reduce the heat resistance, so that the energy transfer

from/to the heaters can be quick, while glass/polymer is used on the other side, exposed to the ambient air to increase insulation so that the energy loss can be minimised.

In a microfluidic device, especially within a microdroplet, mixing is usually achieved via diffusion. Mass diffusion is a statistical transport phenomenon caused by a concentration gradient, which can be described by the Fick's law:

$$\mathbf{V} = -D\nabla(\ln C), \tag{3}$$

where $\mathbf{V}$ is the diffusion velocity, C is concentration and D is the coefficient of diffusivity. This coefficient varies with temperature as well.

The thermal mass, which is a measure of the ability of a material to store thermal energy, can be described by $\rho \, c_p$, where c_p is the specific heat. A moving fluid with a high thermal mass will carry more thermal energy than a fluid with a low thermal mass, so that it will have a larger impact on the temperature distribution of the surrounding medium. In other words, the fluid with a large thermal mass will take a longer time to heat up or cool down. Since water usually has a larger thermal mass than oil, it is better to use an oil phase as the carrier fluid in the PCR process.

6.2. Flow characteristics

Fluid flow in microfluidic devices is usually at a low speed so that the viscous force is more important than the inertia force, which can be classified by a non-dimensional Reynolds number Re:

$$Re = \frac{\rho u L}{\mu}, \tag{4}$$

where ρ is fluid density, and L is the characteristic length scale, e.g., channel depth or width. When Re is smaller than 100, the flow is usually laminar. Very often, the Reynolds number for microflow is smaller than unity, so that the flow is in the creeping flow regime and the inertia effect may not be significant. For flow with heat transfer, the non-dimensional parameter Prandtl number is important, which is defined as the ratio of viscous and thermal diffusion rates, i.e.

$$Pr = \frac{\mu c_p}{\kappa} \tag{5}$$

Small Pr indicates that heat diffuses quickly, in comparison with momentum diffusion. The typical number for Pr is 0.7–0.8 for air, while it is about 7 for water.

The fluid flow with heat transfer is described by the Navier–Stokes–Fourier equations, which are conservation equations for mass, momentum and energy. For a typical microfluidic PCR device using the common pressure-pumping method to drive the PCR mixture through the various thermal cycles, the flow velocity profile is parabolic, with no motion at the surface. For better illustration, a two-dimensional channel is used as an example. At the wall surface, fluid has zero velocity, while it has maximum velocity at the centre. The averaged velocity is 2/3 of the maximum velocity and a large proportion of the cross-sectional area, which is close to the surface, has significantly smaller velocity than the averaged velocity. The direct consequence is that the DNA sample and reagents, which are assumed distributed evenly in the cross-sectional area, spend a very different time in each thermal cycle, depending on their cross-sectional position. Therefore, optimized flow rates to ensure appropriate times for denaturation, annealing and extension become impossible. If a droplet is used to contain all the DNA sample and reagents, then the sample and reagents will move with the droplet at the same velocity, which is easy for optimization of thermal-cycling times.

Not as the classical Graetz problem, the thermal development length, which needs to be minimised to have a short transition

length between high/low temperature zones, does not simply depend on the Prandtl number and Reynolds number, due to the coupled nature of the solid–fluid thermal interactions. Generally, a small Reynolds number and thermal mass will lead to a shorter thermal development length. Since the microchannel has a large surface area/volume ratio, the heat transferred from/to the surface is very rapid.

Properly choosing the computational domain and the boundary conditions for the fluid flow in the microchannel is most important but difficult to do when using computational software. In the simulation, researchers usually need to know the temperature and velocity fields of the flowfield in microchannels, which is a very small proportion of the whole chip. To resolve the flowfield in 3 dimensions, the computational cost would be very large, due to the amount of computational grids required for the computational domain which may include the flowfield in channels, the whole chip and the surrounding environment. Therefore, simulating one thermal cycle has been adopted by some researchers, e.g., [47,95]. The underlying assumption is that each thermal cycle is identical, which is not always true, especially at a large flow rate as discovered by Mohr et al. [24,43]. For a deeper insight into this subject, specialty text books, such as Versteeg and Malalasekera [96] can be referred to.

7. Future perspective for microfluidic PCR in droplets

Although utilization of microdroplet technology for PCR is only emerging, the principle and potentials have been demonstrated by recent research work, e.g., [89–93]. To enable users to embrace this technology, future development in system integration, device design optimization, device manufacture, and system automation will be essential. System integration may take advantage of recent technological advances in microelectronics and micro-optics to have better capability for online detection and droplet manipulation. All the required processing steps for PCR such as droplet generation can be achieved on chip, so that PCR can become an integrated functional component for a μTAS device. In addition, device design optimization is important for performance enhancement and reduction of running cost. Although bespoke design may still be necessary, many components may be standardised to reduce the fabrication and maintenance costs. Until now, the microfluidic technology has not yet revolutionized the current practice in biological and chemical analyses. One of the reasons is that the device is not easy for users to operate. Future research work on device automation to reduce (or even eliminate) user interference is critical to evolve this technology out of research laboratories.

8. Conclusions

Microfluidic technology has dramatically changed conventional PCR for DNA amplification. Due to its small thermal mass, microfluidic PCR can greatly reduce the time for PCR processing which is critical for instant medical diagnosis and in-field detection. The potential for massive parallel operation is convenient and can increase throughput dramatically. Because only a small amount of expensive reagents are required, experimental costs can be significantly reduced. The PCR inhibition and carryover contamination often occur in continuous-flow microPCRs, which can be overcome by using droplet technology. PCR in droplets can enable single DNA molecule and single-cell amplification, and can eliminate the preference for amplifying short fragments and the production of short chimeric molecules associated with single-phase PCR. Although the development of droplet-based continuous-flow microPCR is still in the early stages, its great potential for becoming the next generation PCR for DNA amplification has recently been demonstrated.

References

[1] BCC Research, Microfluidics Technology (2006).
[2] S.C. Terry, PhD thesis, Stanford University, USA (1975).
[3] J.M. Bartlett, D. Stirling, Methods Mol. Biol. 226 (2003) 3.
[4] P.-A. Auroux, D.R. Reyes, D. Iossifidis, A. Manz, Anal. Chem. 74 (2002) 2637.
[5] P.-A. Auroux, Y. Koc, A. deMello, A. Manz, P.J.R. Day, Lab Chip 4 (2004) 534.
[6] T. Vilkner, D. Janasek, A. Manz, Anal. Chem. 76 (2004) 3373.
[7] L. Chen, A. Manz, P.J.R. Day, Lab Chip. 7 (2007) 1413.
[8] M.A. Northrup, M.T. Ching, R.M. White, R.T. Watson, Transducers 93 (1993) 924.
[9] C.T. Wittwer, M.G. Hermann, in: M.A. Innis, D.H. Gelfand, J.J. Sninsky (Eds.), PCR Applications: Protocols for Functional Genomics, Academic, San Diego, 1999, pp. 211–229.
[10] Y. Sun, C. Yien, C. Kwok, Anal. Chim. Acta 556 (2006) 80.
[11] C.S. Zhang, J.L. Xu, W.L. Ma, W.L. Zheng, Biotech. Adv. 24 (2006) 243.
[12] C. Zhang, D. Xing, Y. Li, Biotech. Adv. 25 (2007) 483.
[13] C.S. Zhang, D. Xing, Nucleic Acids Res. 35 (2007) 4223.
[14] S.-E. Ong, S. Zhang, H. Du, Y. Fu, Frontiers Biosci. 13 (2008) 2757.
[15] P. Wilding, M.A. Shoffner, L.J. Kricka, Clin. Chem. 40 (1994) 1815.
[16] P. Belgrader, W. Benett, D. Hadley, J. Richards, P. Stratton, R. Mariella, F. Milanovich, Science 284 (1999) 449.
[17] A. Gulliksen, L. Solli, F. Karlsen, H. Rogne, E. Hovig, T. Nordstrom, R. Sirevag, Anal. Chem. 76 (2004) 9.
[18] T. Ohashi, H. Kuyama, N. Hanafusa, Y. Togawa, Biomed. Microdevices 9 (2007) 695.
[19] H. Nakano, K. Matsuda, M. Yohda, T. Nagamune, I. Endo, T. Yamane, Biosci. Biotechnol. Biochem. 58 (1994) 349.
[20] M.U. Kopp, A.J. de Mello, A. Manz, Science 280 (1998) 1046.
[21] J. Chiou, P. Matsudaira, A. Sonin, D. Ehrlich, Anal. Chem. 73 (2001) 2018.
[22] Z.Y. Chen, S.Z. Qian, W.R. Abrams, D. Malamud, H.H. Bau, Anal. Chem. 76 (2004) 3707.
[23] H. Wang, J. Chen, L. Zhu, H. Shadpour, M.L. Hupert, S.A. Soper, Anal. Chem. 78 (2006) 6223.
[24] S. Mohr, Y.-H. Zhang, A. Macaskill, P.J.R. Day, R.W. Barber, N.J. Goddard, D.R. Emerson, P.R. Fielden, Microfluid. Nanofluid. 3 (2007) 611.
[25] M.Q. Bu, M. Tracy, G. Ensell, J.S. Wilkinson, A.G.R. Evans, J. Micromech. Microeng. 13 (2003) S125.
[26] P.A. Auroux, P.J.R. Day, A. Manz, Proceedings of the 9th International Conference on Miniaturized Systems for Chemistry and Life Sciences, Boston, MA, USA, 2005.
[27] W. Wang, Z.-X. Li, R. Luo, S.-H. Lü, A.-D. Xu, Y.-J. Yang, J. Micromech. Microeng. 15 (2005) 1369.
[28] J. Liu, M. Enzelberger, S. Quake, Electrophoresis 23 (2002) 1531.
[29] J. West, B. Karamata, B. Lillis, J.P. Gleeson, J. Alderman, J.K. Collins, W. Lane, A. Mathewson, H. Berney, Lab Chip 2 (2002) 224.
[30] D.J. Sadler, R. Changrani, P. Roberts, C.F. Chou, F. Zenhausern, IEEE Trans. Compon. Pack. Technol. 26 (2003) 309.
[31] N. Park, S. Kim, J.H. Hahn, Anal. Chem. 75 (2003) 6029.
[32] N. Crews, C. Wittwer, B. Gale, Biomed. Microdevices 10 (2008) 187.
[33] N.A. Friedman, D.R. Meldrum, Anal. Chem. 70 (1998) 2997.
[34] C.J. Bruckner-Lea, T. Tsukuda, B. Dockendorff, J.C. Follansbee, M.T. Kingsley, C. Ocampo, J.R. Stults, D.P. Chandler, Anal. Chim. Acta 469 (2002) 129.
[35] P. Belgrader, C.J. Elkin, S.B. Brown, S.N. Nasarabadi, R.G. Langlois, F.P. Milanovich, B.W. Colston Jr., Anal. Chem. 75 (2003) 3446.
[36] I. Schneegaß, J.M. Köhler, Rev. Mol. Biotechnol. 82 (2001) 101.
[37] I. Schneegaß, R. Bräutigam, J.M. Köhler, Lab Chip 1 (2001) 42.
[38] K. Sun, A. Yamaguchi, Y. Ishida, S. Matsuo, H. Misawa, Sens. Actuators B Chem. 84 (2002) 283.
[39] J. Felbel, I. Bieber, J. Pipper, J.M. Köhler, Proc. SPIE 4937 (2002) 34.
[40] T. Fukuba, T. Yamamoto, T. Naganuma, T. Fujii, Chem. Eng. J. 101 (2004) 151.
[41] P.J. Obeid, T.K. Christopoulos, H.J. Crabtree, C.J. Backhouse, Anal. Chem. 75 (2003) 288.
[42] P.J. Obeid, T.K. Christopoulos, Anal. Chim. Acta 494 (2003) 1.
[43] S. Mohr, Y.-H. Zhang, A. Macaskill, P.J.R. Day, R.W. Barber, N.J. Goddard, D.R. Emerson, P.R. Fielden, Proceedings of the 4th International Conference on Nanochannels, Microchannels and Minichannels, Limerick Ireland. pp. Paper 96131 June 2006.
[44] Y. Sun, Y.C. Kwoka, N.T. Nguyen, Lab Chip 7 (2007) 1012.
[45] M. Krishnan, V.M. Ugaz, M.A. Burns, Science 298 (2002) 793.
[46] D. Braun, N.L. Goddard, A. Libchaber, Phys. Rev. Lett. 91 (2003) 1581031.
[47] M. Hashimoto, P.-C. Chen, M.W. Mitchell, D.E. Nikitopoulos, S.A. Soper, M.C. Murphy, Lab Chip 4 (2004) 638.
[48] S. Li, D.Y. Fozdar, M.F. Ali, H. Li, D. Shao, D.M. Vykoukal, J. Vykoukal, P.N. Floriano, M. Olsen, J.T. McDevitt, P.R.C. Gascoyne, J. MEMS 15 (2006) 223.
[49] M. Yang, R. Pal, M.A. Burns, J. Micromech. Microeng. 15 (2005) 221.
[50] M. Hashimoto, F. Barany, F. Xu, S.A. Soper, Analyst 132 (2007) 913.
[51] T. Nakayama, Y. Kurosawa, S. Furui, K. Kerman, M. Kobayashi, S.R. Rao, Y. Yonezawa, K. Nakano, A. Hino, S. Yamamura, Y. Takamura, E. Tamiya, Anal. Bioanal. Chem. 386 (2006) 1327.
[52] O. Frey, S. Bonneick, A. Hierlemann, J. Lichtenberg, Biomed. Microdevices 9 (2007) 711.
[53] J.S. Marcus, W.F. Anderson, S.R. Quake, Anal. Chem. 78 (2006) 956.
[54] A. Gonzalez, R. Grimes, E.J. Walsh, T. Dalton, M. Davies, Biomed. Microdevices 9 (2007) 261.
[55] K. Kolari, R. Satokari, K. Kataja, J. Stenman, A. Hokkanen, Sens. Actuators B 128 (2008) 442.

[56] W. Wang, H.B. Wang, Z.X. Li, Z.Y. Guo, J. Biomed. Mater. Res. A 77 (2006) 28.
[57] P. Wilding, M.A. Shoffner, J. Cheng, G.E. Hvichia, L.J. Kricka, Clin. Chem. 41 (1995) 1367.
[58] M.A. Shoffner, J. Cheng, G.E. Hvichia, L.J. Kricka, P. Wilding, Nucleic Acids Res. 24 (1996) 375.
[59] T.B. Taylor, E.S. Winn-Deen, E. Picozza, T.M. Woudenberg, M. Albin, Nucleic Acids Res. 25 (1997) 3164.
[60] L.J. Kricka, P. Wilding, Anal. Bioanal. Chem. 377 (2003) 820.
[61] I. Erill, S. Campoy, N. Erill, J. Barbé, J. Aguiló, Sens. Actuators B Chem. 96 (2003) 685.
[62] M. Krishnan, D.T. Burke, M.A. Burns, Anal. Chem. 76 (2004) 6588.
[63] J. Felbel, I. Bieber, J. Pipper, J.M. Köhler, Chem. Eng. J. 101 (2004) 333.
[64] N.J. Panaro, X.J. Lou, P. Fortina, L.J. Kricka, P. Wilding, Biomed. Microdevices 6 (2004) 75.
[65] J.A. Kim, J.Y. Lee, S. Seong, S.H. Cha, S.H. Lee, J.J. Kim, T.H. Park, Biochem. Eng. J. 29 (2006) 91.
[66] A.R. Prakash, M. Amrein, K.V.I.S. Kaler, Microfluid. Nanofluid. 4 (2008) 295.
[67] Y.-M. Xia, Z.-S. Hua, O. Srivannavit, A.B. Ozel, E. Gulari, J. Chem. Technol. Biotechnol. 82 (2007) 33.
[68] L. Chen, J. West, P.-A. Auroux, A. Manz, P.J.R. Day, Anal. Chem. 79 (2007) 9185.
[69] V. Taly, B.T. Kelly, A.D. Griffiths, ChemBioChem 8 (2007) 263.
[70] A. Günther, K.F. Jensen, Lab Chip 6 (2006) 1487.
[71] B.T. Kelly, J.-C. Baret, V. Taly, A.D. Griffiths, Chem. Commun. (2007) 1773.
[72] S.-Y. Teh, R. Lin, L.-H. Hung, A.P. Lee, Lab Chip 8 (2008) 198.
[73] A. Huebner, S. Sharma, M. Srisa-Art, F. Hollfelder, J.B. Edel, A.J. deMello, Lab Chip 8 (2008) 1244.
[74] M. Margulies, M. Egholm, W.E. Altman, S. Attiya, J.S. Bader, L.A. Bemben, J. Berka, M.S. Braverman, Y.J. Chen, Z. Chen, S.B. Dewell, L. Du, J.M. Fierro, X.V. Gomes, B.C. Godwin, W. He, S. Helgesen, C.H. Ho, G.P. Irzyk, S.C. Jando, M.L. Alenquer, T.P. Jarvie, K.B. Jirage, J.B. Kim, J.R. Knight, J.R. Lanza, J.H. Leamon, S.M. Lefkowitz, M. Lei, J. Li, K.L. Lohman, H. Lu, V.B. Makhijani, K.E. McDade, M.P. McKenna, E.W. Myers, E. Nickerson, J.R. Nobile, R. Plant, B.P. Puc, M.T. Ronan, G.T. Roth, G.J. Sarkis, J.F. Simons, J.W. Simpson, M. Srinivasan, K.R. Tartaro, A. Tomasz, K.A. Vogt, G.A. Volkmer, S.H. Wang, Y. Wang, M.P. Weiner, P. Yu, R.F. Begley, J.M. Rothberg, Nature 437 (2005) 376.
[75] J. Shendure, G.J. Porreca, N.B. Reppas, X. Lin, J.P. McCutcheon, A.M. Rosenbaum, M.D. Wang, K. Zhang, R.D. Mitra, G.M. Church, Science 309 (2005) 1728.
[76] M. Li, F. Diehl, D. Dressman, B. Vogelstein, K.W. Kinzler, Nat. Methods 3 (2006) 95.
[77] K. Zhang, J. Zhu, J. Shendure, G.J. Porreca, J.D. Aach, R.D. Mitra, G.M. Church, Nat. Genet. 38 (2006) 382.
[78] J.G. Wetmur, M. Kumar, L. Zhang, C. Palomeque, S. Wallenstein, J. Chen, Nucleic Acids Res. 33 (2005) 2615.
[79] D. Dressman, H. Yan, G. Traverso, K.W. Kinzler, B. Vogelstein, Proc. Natl. Acad. Sci. U.S.A. 100 (2003) 8817.
[80] T. Kojima, Y. Takei, M. Ohtsuka, Y. Kawarasaki, T. Yamane, H. Nakano, Nucleic Acids Res. 33 (2005) e150.
[81] R. Williams, S.G. Peisajovich, O.J. Miller, S. Magdassi, D.S. Tawfik, A.D. Griffiths, Nat. Methods 3 (2006) 545.
[82] S. Hardt, D. Dadic, F. Doffing, K.S. Drese, G. Münchow, O. Sörensen, Nanotechnology 1 (2004) 55.
[83] M. Curcio, J. Roeraade, Anal. Chem. 75 (2003) 1.
[84] T. Nisisako, T. Torii, T. Higuchi, Lab Chip 2 (2002) 24.
[85] A. Musyanovych, V. Mailnder, K. Landfester, Biomacromolecules 6 (2005) 1824.
[86] M. Nakano, N. Nakai, H. Kurita, J. Komatsu, K. Takashima, S. Katsura, A. Mizuno, J. Biosci. Bioeng. 99 (2005) 293.
[87] K.D. Dorfman, M. Chabert, J.-H. Codarbox, G. Rousseau, P. de Cremoux, J.-L. Viovy, Anal. Chem. 77 (2005) 3700.
[88] M. Chabert, K.D. Dorfman, P. de Cremoux, J. Roeraade, J.-L. Viovy, Anal. Chem. 78 (2006) 7722.
[89] N.R. Beer, B.J. Hindson, E.K. Wheeler, S.B. Hall, K.A. Rose, I.M. Kennedy, B.W. Colston, Anal. Chem. 79 (2007) 8471.
[90] N.R. Beer, E.K. Wheeler, L. Lee-Houghton, N. Watkins, S. Nasarabadi, N. Hebert, P. Leung, D.W. Arnold, C.G. Bailey, B.W. Colston, Anal. Chem. 80 (2008) 1854.
[91] H. Tsuchiya, M. Okochi, N. Nagao, M. Shikida, H. Honda, Sens. Actuators B 130 (2008) 583.
[92] M.M. Kiss, L. Ortoleva-Donnelly, N.R. Beer, J. Warner, C.G. Bailey, B.W. Colston, J.M. Rothberg, D.R. Link, J.H. Leamon, Anal. Chem. 80 (2008) 8975.
[93] Y. Schaerli, R.C. Wootton, T. Robinson, V. Stein, C. Dunsby, M.A.A. Neil, P.M.W. French, A.J. deMello, C. Abell, F. Hollfelder, Anal. Chem. 81 (2009) 302.
[94] Q. Zhang, W. Wang, H. Zhang, Y. Wang, Sens. Actuators B 82 (2002) 75.
[95] P.C. Chen, D.E. Nikitopoulos, S.A. Soper, M.C. Murphy, Biomed. Microdevices 10 (2008) 141.
[96] H.K. Versteeg, W. Malalasekera, An Introduction to Computational Fluid Dynamics, Pearson Education Ltd., London, 2007.